Thermotropic Properties of Bilayers Containing Branched-Chain Phospholipids. Calorimetric, Raman, and ^{31}P NMR Studies†

John R. Silvius* and Michael Lyons‡
Department of Biochemistry, McGill University, Montreal, Québec H3G 1Y6, Canada
Philip L. Yeagle
Department of Biochemistry, State University of New York at Buffalo, Buffalo, New York 14214
Timothy J. O'Leary*
Laboratory of Chemical Physics, National Institute of Arthritis, Diabetes and Digestive and Kidney Diseases, National Institutes of Health, Bethesda, Maryland 20205
Received January 15, 1985

ABSTRACT: Diisopalmitoylphosphatidylcholine (DIPPC), -phosphatidylethanolamine (DIPPE), and -phosphatidylglycerol (DIPPG) have been synthesized, and the structures of aqueous dispersions of these lipids have been examined by high-sensitivity differential scanning calorimetry, ^{31}P nuclear magnetic resonance, and Raman spectroscopy. DIPPC at temperatures below 23.1 °C readily forms a gel phase with the acyl chains packed in an orthorhombic subcell. Above this temperature, this "orthorhombic" phase converts directly to the liquid-crystalline phase. The phase diagram for the system DIPPC–dipalmitoyl-PC (DIPPC–DPPC) shows that the gel phases formed by either lipid can accommodate only limited amounts of the other species and suggests that the low-temperature orthorhombic phase of DIPPC is distinct in its structure from the "subgel" phase of DPPC. DIPPE forms a well-ordered gel phase only in samples that are equilibrated at low temperatures for long times (approximately days to weeks) or at very high lipid concentrations. However, this lipid readily forms an "intermediate" phase with a very disordered acyl chain packing upon cooling from the liquid-crystalline state. Mixtures of DIPPE with DIPPG exhibit similar thermotropic properties. Hydrated DIPPE appears to be stable in the lamellar phase up to at least 98 °C, while di-*cis*- and di-*trans*-9-hexadecenoyl-PE convert to the hexagonal II phase at 43.5 and 92.5 °C, respectively. We discuss the relevance of these results to the structure and stability of bacterial membranes containing branched-chain acyl lipids.

While the membrane lipids of higher organisms contain almost exclusively linear acyl and alkyl hydrocarbon chains, the membrane lipids of a variety of prokaryotes contain large amounts of branched acyl chains (Kaneda, 1977). Other prokaryotes, whose membrane lipids normally contain exclusively linear acyl chains, will readily incorporate large amounts of branched-chain fatty acids into their membrane lipids if such acids, or their precursors, are added to the growth medium (McElhaney & Tourtellotte, 1969; Rodwell & Peterson, 1971; Silbert et al., 1973; Saito & McElhaney, 1977; Saito et al., 1977; Silvius & McElhaney, 1978). It has been demonstrated that in some organisms, such as *Escherichia coli*, branched acyl chains can replace the normal complement of cis-unsaturated acyl chains in the membrane lipids without loss of cell viability (Silbert et al., 1973). In certain other organisms, such as *Mycoplasma* strain Y and *Acholeplasma laidlawii B*, the linear acyl chains normally found in the membrane lipids can be entirely replaced by any of a number of methyl-branched fatty acids while maintaining high levels of cell growth (Rodwell & Peterson, 1971; Silvius & McElhaney, 1978). Branched-chain fatty acids thus appear to be able to support membrane function in a variety of prokaryotic organisms at least as well as do straight-chain-saturated or cis-unsaturated species.

Previous studies on the physical properties of iso- and anteisobranched phosphatidylcholines (PC's)[1] have suggested that some physical properties of a branched-chain lipid may be intermediate between those of the saturated *n*-acyl and the cis-unsaturated *n*-acyl species of the same carbon number (Silvius & McElhaney, 1979, 1980a; Kannenberg et al., 1983). However, natural membranes containing branched-chain lipids have been found to exhibit some unusual physical properties, particularly at low temperatures, where these membranes form a lipid gel phase that appears to be much less well-ordered than the gel phase in membranes containing straight-chain fatty acids (Haest et al., 1974; Verkleij & Ververgaert, 1975; Halverson et al., 1978; Legendre et al., 1980; Silvius & McElhaney, 1980b; Bouvier et al., 1981). In this study, we have combined scanning calorimetry, Raman spectroscopy, and ^{31}P NMR to examine in detail the structure and the thermotropic behavior of aqueous dispersions of a branched-chain PC and of the corresponding PE and PG species, whose head groups represent the major phospholipid species in bacterial membranes containing iso- and anteisobranched lipids (Kaneda, 1977). Our results indicate that many of the properties of pure branched-chain lipids are quite different

† This work was supported by grants from the Medical Research Council (ME-7580 and MA-7776) and le Fonds de la recherche en santé du Québec (820040) to J.R.S. and from the National Institutes of Health (GM-28120) to P.L.Y.
‡ Present address: Department of Physics, The University of British Columbia, Vancouver, British Columbia, Canada V6T 1W5.

[1] Abbreviations: DIP, diisopalmitoyl; DP, dipalmitoyl; EDTA, ethylenediaminetetraacetic acid trisodium salt; NMR, nuclear magnetic resonance; PC, 1,2-diacyl-*sn*-glycero-3-phosphocholine; PE, 1,2-diacyl-*sn*-glycero-3-phosphoethanolamine; PG, 1,2-diacyl-*sn*-glycero-3-phospho-1′-glycerol; T_c, gel to liquid-crystalline transition temperature; TES, *N*-[tris(hydroxymethyl)methyl]-2-aminoethanesulfonic acid; T_H, lamellar to hexagonal II transition temperature; TLC, thin-layer chromatography; FR, Fermi resonance.

0006-2960/85/0424-5388$01.50/0

from those of either saturated or unsaturated straight-chain lipids, and they provide some insight into the unusual behavior of branched-chain lipids in natural membranes.

Materials and Methods

Materials. 11-Bromo-1-undecanol, 1-bromo-3-methylbutane, and 4-pyrrolidinopyridine were obtained from Aldrich (Milwaukee, WI). L-α-Glycerophosphocholine (grade I) was obtained as the cadmium chloride adduct from Sigma (St. Louis, MO). Dipalmitoylphosphatidylcholine (grade I, 99%) was also obtained frm Sigma and was judged to be of acceptable purity by TLC and by calorimetry, which gave comparable thermograms for the product as used directly and after preparative thin-layer chromatography and/or acetone precipitation. All solvents were redistilled, and all organic and inorganic reagents were of at least reagent grade.

Synthesis of Isopalmitic Acid. 11-Bromo-1-undecanol (75 mmols) was converted to its tetrahydropyranyl ether (Miyashita et al., 1977) and condensed with the Grignard reagent prepared from 1-bromo-3-methylbutane (115 mmol), using dilithium tetrachlorocuprate as catalyst, as described by Baer & Carney (1976). The crude products were deprotected (Miyashita et al., 1977), refluxed with 25 g of thiourea and 250 mL of ethanol for 1 h, and then partitioned 3 times between chloroform and 0.3 M HCl and methanol (1:1 v/v) to remove unreacted bromo alcohol as its thiouronium derivative. The alcohol was then oxidized to the carboxylic acid with chromic acid in acetone (Gunstone & Ismail, 1967) and purified by partitioning between hexane and aqueous alkali plus methanol (1:1 v/v) followed by silicic acid column chromatography and two recrystallizations from 85:15 (v/v) hexane/chloroform. Isopalmitic acid was obtained in 55% yield (based on protected bromoundecanol) and was shown by gas–liquid chromatography to be ≥99.8% pure.

Lipid Synthesis. Phosphatidylcholines were prepared from anhydrous glycerophosphocholine–cadmium chloride adduct and fatty acid anhydrides, using 4-pyrrolidinopyridine as catalyst, as described previously (Silvius & Gagné, 1984). Phosphatidylethanolamines were prepared by phospholipase D catalyzed transphosphatidylation of phosphatidylcholine (Comfurius & Zwaal, 1977) and purified as described in Silvius & Gagné (1984). Diisopalmitoylphosphatidylglycerol was also prepared by enzymatic transphosphatidylation of diisopalmitoyl-PC but was purified by preparative TLC, then precipitated from chloroform solution with an excess of cold acetone, and finally converted to the sodium salt essentially as described by Papahadjopoulos & Miller (1967).

Calorimetry. Lipid samples (1–5 μmol) were lyophilized from benzene and redispersed in 10 mM histidine or TES and 1 mM EDTA, pH 7.4, above their phase transition temperatures. The samples were cooled at ≤0.3 °C/min to 2 °C, incubated at this temperature for varying periods, as indicated in the text, and then transferred to the calorimeter at ≤5 °C. Calorimetry was performed on a Microcal MC-1 high-sensitivity differential scanning calorimeter, at a scan rate of 12 °C/h, as described previously (Silvius & Gagné, 1984). Lipid was assayed as described by Lowry & Tinsley (1974) with the modification that samples were digested for 6 h to ensure complete release of organic phosphorus as phosphate.

Raman Spectroscopy. Raman spectra of DIPPC and DIPPE, except for those spectra explicitly used to generate temperature profiles, were acquired on a Spex Ramalog 6 spectrometer system which has been described previously (O'Leary & Levin, 1984a). Laser excitation at 514.5 nm provided from 200 mW (dispersions) to 400 mW (polycrystalline samples) of power at the sample. The temperature-dependent spectra of DIPPE dispersions were acquired on a Spex Triplemate Raman spectrometer equipped with two 600 grooves/mm gratings in the filter stage and a 1200 grooves/mm grating in the spectrographic stage. An EG & G Model 1420 intensified silicon photodiode array detector was coupled through the detector controller to a laboratory PDP 11-70 computer for data storage and manipulation. Excitation with 514.5-nm light provided ~30 mW of power at the sample. In both systems, spectra were acquired at an instrumental resoltuion of 5 cm^{-1}.

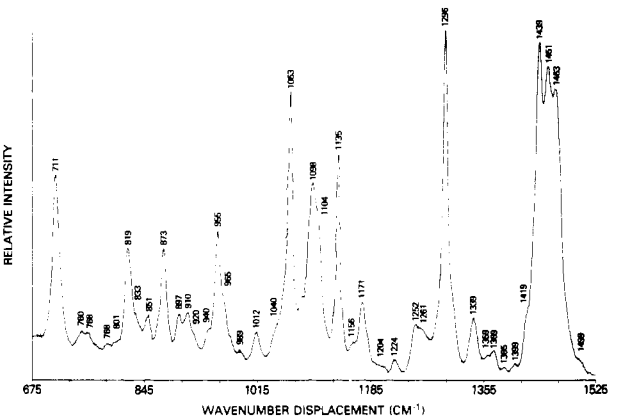

FIGURE 1: Raman spectrum for an unhydrated sample of DIPPC. Experimental details are given under Materials and Methods, and spectral band assignments are given in Table I.

Lipid dispersions for Raman experiments were prepared by adding distilled water to the phospholipid to form a 25% (w/w) lipid/water dispersion. This sample was cycled between 22 and 50 °C multiple times with repeated mechanical agitation. The resulting dispersions were then sealed in 1.25-mm Kimex glass capillary tubes and allowed to remain at room temperature for 1–2 days and at 4 °C for 3–4 days prior to acquiring spectra. Temperature control during data acquisition was provided by placing the sample capillary tube in a thermostatically regulated brass mount.

^{31}P nuclear magnetic resonance spectra were obtained on a JEOL FX 270 Fourier-transform NMR spectrometer at 109 MHz, as described elsewhere (Abidi & Yeagle, 1984).

Results

Raman Spectral Assignments for DIPPC and DIPPE. Raman spectra of anhydrous polycrystalline DIPPC and DIPPE are shown in Figures 1 and 2, respectively; the frequencies and vibrational assignments of major features are found in Table I. In general, the assignments are similar to those of Akutsu & Kyogoku (1975) and O'Leary et al. (1984a), and thus the rationale behind these assignments will not be discussed here. However, several prominent differences between these spectra and those of the straight-chain analogues, DPPC and DPPE, are apparent. For example, while DPPC exhibits weak features at 824 cm^{-1} due to an O–P–O antisymmetric stretching mode, the spectra of both DIPPE and DIPPC show a strong feature at 819–821 cm^{-1}, which is also observed in branched-chain alkanes (Dolish et al., 1974). We attribute this feature to an acyl chain CH_3 rocking mode, which is probably coupled to C–C stretching and C–C–C bending vibrations. The appearance of the acyl chain CH_3 rocking mode at 819–821 cm^{-1} accounts for the absence of strong vibrational features at ~892 cm^{-1}, where the DPPC acyl chain CH_3 rocking mode appears.

The vibrational feature present at 1451 cm^{-1} in DIPPC, but not in DPPC, clearly originates from the manifold of CH_2 deformation modes. While such a feature is only very weakly

Table I: Vibrational Frequencies and Assignments for DIPPC and DIPPE in the 675–1525 and 2800–3100 cm^{-1} Regions

DIPPC frequency (cm^{-1})	DIPPC relative intensity[a]	DIPPE frequency (cm^{-1})	DIPPE relative intensity[a]	assignment
3091	9			choline CH_3 symmetric stretch
2956	37	2958	42	acyl chain CH_3 asymmetric stretch
2936	39	2931	41	CH_3 symmetric stretch in FR with 2870 cm^{-1} overtone and acyl chain CH_2 in FR with CH_2 symmetric stretching fundamental
2899 sh	53			acyl chain CH_2 in FR with CH_2 symmetric stretching fundamental
2880	100	2880	100	CH_2 antisymmetric stretch
2868 sh	62	2870 sh	67	overtone of CH_3 asymmetric deformation in FR with 2931 cm^{-1} CH_3 symmetric stretch
2845	68	2846	74	CH_2 symmetric stretch
1463	89	1462	77	
1451	95	1451	80	acyl chain CH_2, CH_3 deformation
1438	100	1438	100	
1419	18	1415 sh	15	
1369	6	1368	9	CH_3 symmetric deformation
1339	12	1337	17	head-group CH_2 symmetric deformation
1296	98	1296	94	acyl chain CH_2 twist
1252	15			PO_2^- asymmetric stretch
1224	4	1224	3	head-group CH_2 twist
1171	18	1171	20	acyl chain CH_2 rock and CH_3 rock
1135	62	1135	54	acyl chain all-trans C–C stretch
1104 sh	46			*sn*-1 chain $k = 1$ C–C stretching mode
1098	55	1097	54	*sn*-2 chain $k = 1$ C–C stretching mode, PO_2^- asymmetric stretch (especially PE)
1063	82	1063	73	acyl chain trans C–C stretch
1040	9			glycerol ester C–O stretch
		1019	9	head-group C–C stretch
1012	9			head-group C–C stretch and C–N stretch
965	15			C–N asymmetric stretch
955	39			choline CH_3 rock
		884	16	C–C–N symmetric stretch
819	29	819	36	acyl chain CH_3 rock
760	4	757	16	O–P–O symmetric stretch
711	50			choline C–N symmetric stretch

[a] Features in the 675–1525 cm^{-1} region were normalized to 100 with respect to the 1438 cm^{-1} CH_2 deformation feature. Those in the 2800–3100 cm^{-1} region were normalized to 100 with respect to the 2880 cm^{-1} CH stretching feature.

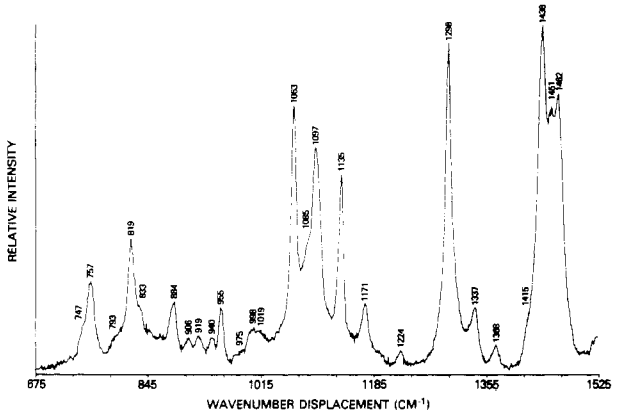

FIGURE 2: Raman spectrum for an unhydrated sample of DIPPE. Spectral band assignments are given in Table I.

present in even-chain phospholipids such as phosphatidylcholine, it is much more apparent in odd-chain ether lipids (W. H. Harris and I. W. Levin, personal communication). This feature may be pronounced in the spectra of DIPPC and DIPPE because the acyl chain *length* in these compounds is odd as a result of the chain branching. The specific origin of the 1451 cm^{-1} band is uncertain, but possible sources include a combination band from CH_2 wagging modes at 719 and 732 cm^{-1}, antisymmetric CH_2 deformation modes, or antisymmetric CH_3 deformation modes from acyl chain or choline methyl groups.

Thermotropic Behavior of DIPPC and DPPC. Heating thermograms recorded for DIPPC samples equilibrated for periods ranging from 2 h to 28 days at 2 °C exhibit a single slightly asymmetrical endotherm at 23.1 °C (Figure 3). The

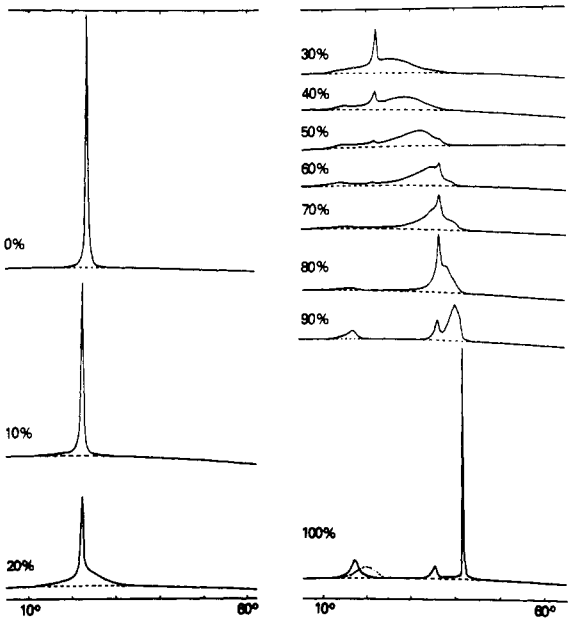

FIGURE 3: Thermograms recorded for mixtures of DIPPC and DPPC containing the indicated molar percentages of DPPC. DIPPC-containing samples were dispersed initially at 45 °C, then cooled to 2 °C at ≤0.2 °C/min, and incubated for 10 days at 2 °C prior to calorimetry. Thermograms are also shown for DPPC samples prepared similarly but incubated for 3 days (solid curve) or 82 days (dashed curve) at 2 °C. Other experimental details are given in the text.

integrated enthalpy of this endothermic transition is 13.8 ± 0.2 kcal mol^{-1} (average of three samples), and its width at half-height is 0.43 °C, roughly double the width of the main transition of pure DPPC. Samples of DPPC equilibrated at

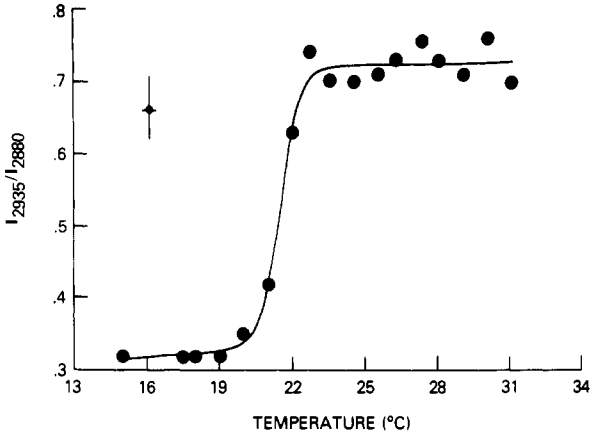

FIGURE 4: Raman peak height intensity ratio I_{2935}/I_{2880} for hydrated DIPPC as a function of temperature. Experimental details are given in the text.

2 °C for 3–7 days show endothermic transitions centered at 18.5 (ΔH = 5.3 ± 0.3 kcal mol^{-1}), 35.4 (ΔH = 1.7 ± 0.2 kcal mol^{-1}), and 41.7 °C (ΔH = 9.5 ± 0.4 kcal mol^{-1}), in agreement with previously reported results (Silvius, 1982; Ruocco & Shipley, 1982a,b). Interestingly, DPPC samples that are incubated for long times (≥7 days) at 2 °C show the gradual emergence of a second subtransition component which is incompletely resolved from the first but appears to be centered at ~21 °C (Figure 3, dashed curve). This component increases with time in a quite reproducible manner, apparently at the expense of the first component, until after ~30 days its amplitude is roughly equal to that of the first component. Similar behavior has been reported recently by Finegold & Singer (1984) for diheptadecanoyl-PC, for which the two components of the subtransition are more fully resolved. Our results suggest that DPPC exhibits two (and perhaps more) subgel phases, which interconvert only over periods of weeks.

The temperature profile of the Raman peak height intensity ratio I_{2935}/I_{2880}, derived from the 2900 cm^{-1} C–H stretching mode region, is shown in Figure 4 for DIPPC. The change in this ratio at the main transition temperatures for various *n*-acyl lipids is proportional to the enthalpy of transition (Huang et al., 1982) and is directly sensitive to the change in the gauche:trans ratio for the acyl chains. The plot shows a phase transition centered at approximately 22 °C, in agreement with the calorimetric results. The change in the I_{2935}/I_{2880} ratio (0.4) is greater than that for pure DPPC (0.3) at the main melting transition, consistent with the significantly larger enthalpy for this transition in the isobranched compound. Spectra taken in the 1375–1525 cm^{-1} CH_2 deformation region show a prominent feature at ~1420 cm^{-1} (Figure 5A) which is indicative of acyl chains packed in an orthorhombic subcell (Boerio & Koenig, 1970; Yellin & Levin, 1977). This feature disappears above the phase transition temperature (Figure 5B). Similarly, the profile and peak frequency of the C=O stretching mode change dramatically when the sample is warmed to temperatures above the phase transitions; the peak frequency of this mode shifts from 1727 cm^{-1} at low temperatures to 1736 cm^{-1} in the liquid-crystalline form. These findings correlate with those seen in the CH_2 deformation region, since the low-temperature C=O spectrum is characteristic of orthorhombically packed phosphatidylcholine chains, while the high-temperature form is representative of hexagonally packed or liquid-crystalline lipids (O'Leary & Levin, 1984b).

Mixtures of DIPPC and DPPC, equilibrated for several days at 2 °C, exhibit complex heating thermograms, as shown in Figure 3. Samples that were equilibrated for shorter times (≤24 h) or analyzed at high-temperature scan rates (5 °C/min) gave thermograms that appeared less complex but were difficult to interpret in terms of a consistent "phase diagram". By contrast, in spite of their complexity, the thermograms observed for well-equilibrated DIPPC–DPPC samples exhibit certain distinctive features from which the DIPPC–DPPC

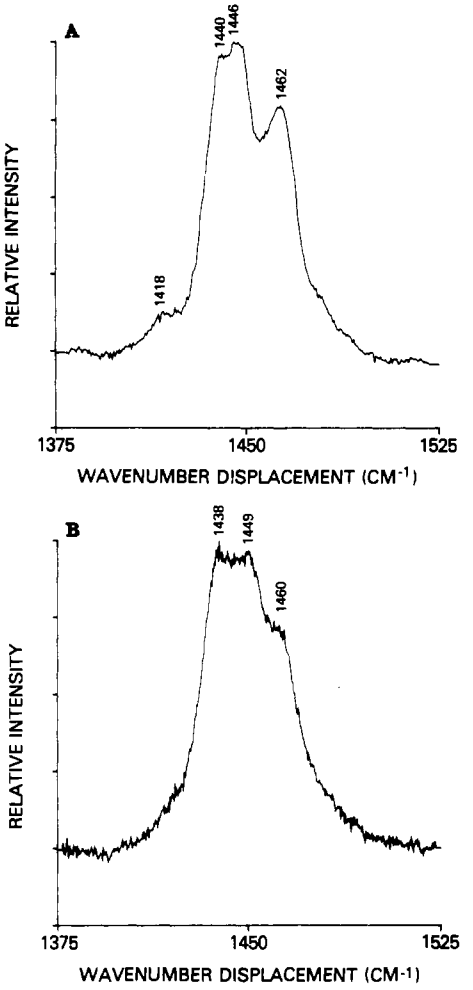

FIGURE 5: (A) Raman spectrum of a hydrated DIPPC dispersion in the 1375–1525 cm^{-1} region. Experimental temperature 20 °C. (B) As in (A) but recorded at 25 °C.

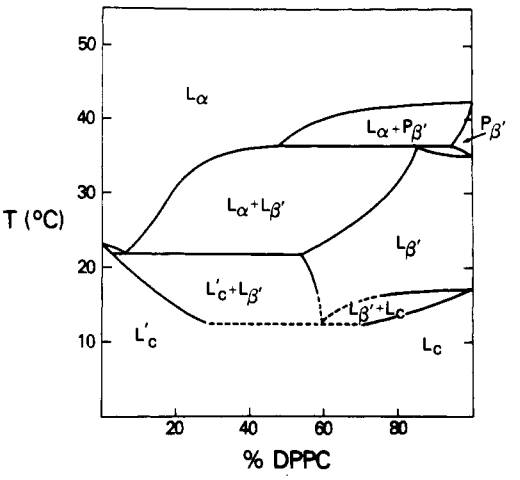

FIGURE 6: Phase diagram derived from calorimetric results for DIPPC–DPPC mixtures. The symbols denoting the various phases are as follows: L_α, liquid-crystalline lamellar; $P_{\beta'}$ and $L_{\beta'}$, nonorthorhombic gel phases of DPPC; L_c and L'_c, orthorhombic phases of DPPC and DIPPC, respectively.

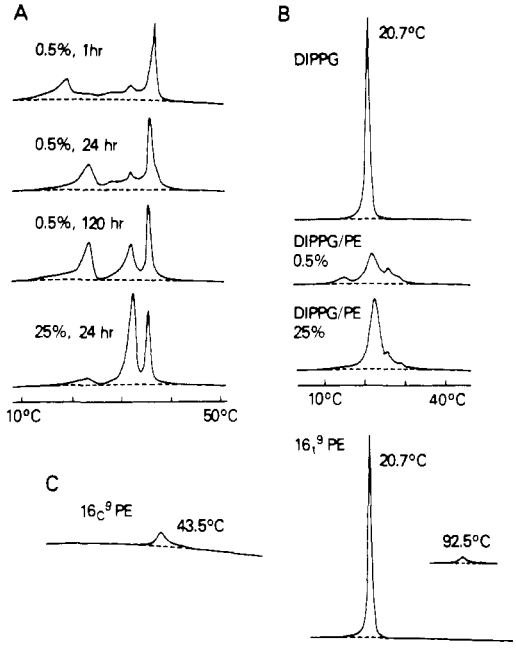

FIGURE 7: (A) Thermograms recorded for DIPPE dispersions prepared at low lipid concentration (0.5 wt %) and preincubated for the indicated times at 2 °C prior to calorimetry (upper three traces) or at 25 wt % lipid and preincubated at 2 °C for 72 h (lowest trace). (B) Thermograms recorded for DIPPG (top trace) and for 1:1 DIPPG/DIPPE mixtures incubated for 24 h at 2 °C after initial warming to 37 °C as a 25 wt % dispersion (middle trace) or a 0.5 wt % dispersion (lower trace). (C) Heating thermograms recorded for dipalmitoleoyl-PE (16c^9-PE) or dipalmitelaidoyl-PE (16t^9-PE). The vertical scale is 4-fold expanded for the former lipid.

phase diagram shown in Figure 6 can readily be constructed, as outlined below.

Sharp endothermic components are observed in the thermograms of various DIPPC–DPPC mixtures at 21.9 and 35.3 °C. The temperatures of these endotherms are quite constant in samples of varying composition, and the endotherms thus appear to represent horizontal boundary lines in the phase diagram. By observing the development of the 35.3 °C endotherm as small amounts of DIPPC are introduced into DPPC, we assign this endotherm to the decomposition of an $L_{\beta'}$ phase, containing ~20% DIPPC, into a liquid-crystalline phase, containing ~50% DIPPC, and a $P_{\beta'}$ phase, containing ~10% DIPPC. Observation of thermograms for mixtures combining DIPPC with low molar fractions of DPPC suggests that the sharp endotherm at 21.9 °C represents a eutectic point at which a mixture containing ~10% DPPC, which exists as a mixture of two gel phases below this temperature, melts to give purely the liquid-crystalline phase. The remainder of the DIPPC–DPPC phase diagram above ~15 °C is then constructed by observing the presence or absence and the amplitudes of these two endotherms, and the onset and completion temperatures for other resolved endotherms or groups of endotherms, in the thermograms of the various DIPPC–DPPC mixtures. For the phase diagram of Figure 6, we have designated solid phases analogous to those formed in pure DPPC by the symbols conventionally used for pure DPPC bilayers: L_c for the subgel phase, L_β, and P_β, for the gel phases interconverting at 35.4 °C, and L_α for the liquid-crystalline phase (Ruocco & Shipley, 1982a). The phase diagram is more difficult to map below 15 °C from the calorimetric data, as the endothermic transitions in this temperature region are small and broad. However, the evolution of these transitions as small amounts of one PC are introduced into the other suggests that the mixing of the two species in the low-temperature region is at best strongly nonideal, with some indication of a miscibility gap between ~40 and ~70 mol % DPPC in DIPPC. We have thus designated the orthorhombic phase of DIPPC as L'_c and not L_c in the phase diagram.

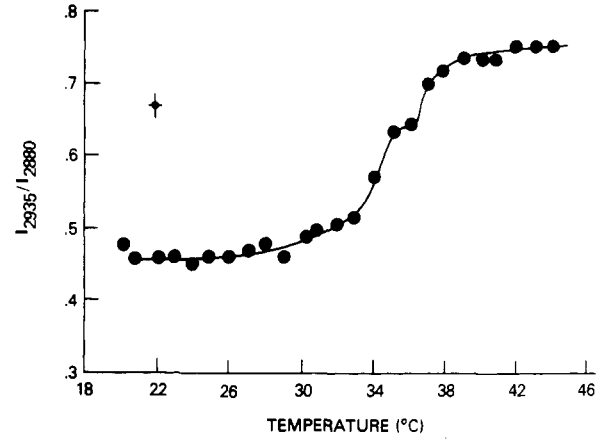

FIGURE 8: Peak height intensity ratio I_{2935}/I_{2880} for a hydrated dispersion of DIPPE as a function of temperature. Experimental details are given in the text.

Thermotropic Behavior of DIPPE. The thermotropic behavior of hydrated DIPPE is strongly influenced by the method of sample preparation, as illustrated in Figure 7A. Dilute samples of DIPPE, incubated briefly at 2 °C after initial hydration at 40 °C, exhibit a prominent broad endotherm with a peak at ~18.5 °C, a very small endotherm at 31.6 °C, and a large, slightly asymmetrical endotherm with a peak at 36.5 °C. A similar thermogram is obtained if the sample is additionally incubated for 12 h at 25 °C before being cooled to 2 °C. After the sample is incubated overnight at 2 °C, the broad 18.5 °C endotherm is largely replaced by a broad endotherm centered at 23.1 °C, and the peak of the high-temperature endotherm has shifted to 35.7 °C, and the peak of the high-temperature endotherm has shifted to 35.7 °C. After 5 days at 2 °C, the positions of the lower and upper endotherms are the same as those observed after overnight incubation, but the endotherm at 31.6 °C has shifted to slightly higher temperatures and increased considerably in amplitude, while the energy content of the 23.1 °C endotherm is slightly reduced. Samples that are equilibrated at a high lipid concentration (25 wt %) for 3 days at 2 °C and then diluted to 0.5 wt % at 2 °C before calorimetric analysis show only a small endotherm at 23.1 °C but a very large endotherm at 32.2 °C and a second large endotherm at 35.3 °C. The enthalpy content of the high-temperature transition is essentially constant regardless of the means of sample preparation, while as already noted, the enthalpy of the transition at ~23 °C is decreased and that of the transition at ~32 °C is increased in samples equilibrated at 2 °C for longer times or at higher lipid concentrations. The enthalpies of the 32.2 and 35.3 °C transitions in samples equilibrated at high lipid concentrations were 6.8 and 3.6 kcal mol^{-1}, respectively, and the total excess specific heat absorbed by such samples between 10 and 45 °C was 11.5 kcal mol^{-1}. No additional endothermic transitions were seen for DIPPE dispersions from 40 °C up to at least 98 °C, regardless of the conditions of sample preparation.

The temperature profile for acyl chain melting of DIPPE, determined from the Raman I_{2935}/I_{2880} peak height intensity ratios, is shown in Figure 8. In agreement with the calorimetric results for DIPPE dispersions preincubated at high lipid concentrations, two transitions are observed, centered at ~34 and ~36.5 °C. These temperatures are slightly different from the calorimetric values (32.2 and 35.3 °C), but it is clear that

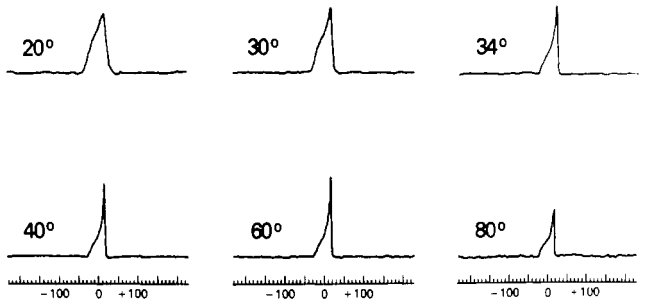

FIGURE 9: ^{31}P NMR spectra recorded for DIPPE (as a ~20 wt % dispersion) at the indicated temperatures. Experimental details are given under Materials and Methods.

the same transitions are observed by both techniques. Since the total change in the I_{2935}/I_{2880} ratio between 30 and 42 °C for DIPPE (0.29) is comparable to that observed for DPPC at the main transition (0.30), it is not surprising that the total excess enthalpy absorbed by DIPPE from 30 to 42 °C (10.4 kcal mol^{-1}) is similar to the enthalpy of the DPPC main transition (9.5 kcal mol^{-1}).

Spectra recorded for DIPPE in the 1375–1525 cm^{-1} deformation region at or below 18 °C show a small shoulder at ~1420 cm^{-1} suggestive of orthorhombic acyl chain packing. This shoulder is not present at 25 °C. By comparing the calorimetric data described above with these Raman spectral results, we tentatively assign the transition observed calorimetrically at 23.1 °C for DIPPE to the onset of rotational motion in lipid acyl chains, as in the alkane rotator phase transition and the subtransition of phosphatidylcholines. While such transitions are associated with a small increase in the number of gauche conformers (Snyder et al., 1981), they produce only minimal changes in the C–H stretching region spectra of phosphatidylcholines (I. W. Levin and C.-H. Huang, unpublished results).

^{31}P NMR spectra were recorded for DIPPE dispersions to ascertain the state of organization of the lipid at various temperatures. The results obtained are summarized in Figure 9. At temperatures below 30 °C, an axially symmetric powder pattern characteristic of a lamellar gel phase is obtained [see, e.g., Cullis et al. (1976)]. Between 30 and 34 °C, a considerable narrowing of the spectral line shape takes place, and further spectral narrowing occurs between 34 and 40 °C, producing a spectrum characteristic of the liquid-crystal phase. The ^{31}P NMR spectra recorded at higher temperatures indicate that DIPPE adopts a purely lamellar organization up to at least 80 °C, the highest temperature examined. This result agrees with the calorimetric findings that DIPPE exhibits no endothermic transitions above 36 °C up to at least 98 °C.

To compare the stabilities of the lamellar phases of PE species with 16-carbon acyl chains of various structures, we also examined the thermotropic behavior of dipalmitoleoyl- and dipalmitelaidoyl-PE. Calorimetric thermograms recorded for hydrated dispersions of these two lipids are shown in Figure 7C. The calorimetric behavior of these two species is simpler and much less dependent on the details of sample equilibration than was found in the case of DIPPE. Dipalmitoleoyl-PE, whose gel to liquid-crystalline phase transition occurs below 0 °C (van Dijick et al., 1976), exhibits a small endotherm at 43.5 °C. ^{31}P NMR showed that this endotherm represents the formation of a hexagonal II phase from a liquid-crystalline lamellar phase (not shown). Dipalmitelaidoyl-PE shows a strongly endothermic transition at 20.7 °C. ($\Delta H = 6.8 \pm 0.4$ kcal mol^{-1}) and a small but quite reproducible endotherm at 92.5 °C. The higher temperature endotherm is likely to represent the lamellar to hexagonal II transition of this lipid. Unfortunately, ^{31}P NMR spectra of good quality could not be collected at temperatures near that of the high-temperature transition. However, no evidence of hexagonal phase formation by dipalmitelaidoyl-PE was found by ^{31}P NMR up to 80 °C, the highest temperature examined by this technique.

Thermotropic Behavior of DIPPG and DIPPE–DIPPG Dispersions. Because PG as well as PE is often a major lipid species in bacterial membranes containing branched-chain acyl lipids, we also examined the calorimetric properties of diisopalmitoyl-PG (DIPPG) and of mixtures of this lipid with DIPPE. As shown in Figure 7B, pure DIPPG (sodium salt) dispersed in distilled water exhibits a single endothermic transition centered at 20.7 °C. For DIPPG dispersed in 200 mM NaCl, 5 mM TES, 5 mM histidine, and 1 mM EDTA, pH 7.4, this transition shifts slightly upward, to 21.2 °C. The integrated enthalpy of this transition is 14.6 kcal mol^{-1}. No differences were seen in the thermograms recorded for DIPPG samples incubated for 1 or 72 h at 0 °C after initial heating to 37 °C.

The heating thermograms obtained for DIPPG–DIPPE mixtures are more complex and more dependent on the details of sample preparation than are those recorded for pure DIPPG, as the traces shown in Figure 7B illustrate. When a 50:50 DIPPG/DIPPE sample is hydrated at 25% (w/v) lipid and incubated for prolonged periods at 2 °C prior to dilution (at 2 °C) to 0.5% (w/v) lipid, the calorimetric thermogram exhibits a broad major endotherm centered at 21.9 °C, plus smaller overlapping endotherms at higher temperatures. The total enthalpy of this composite transition is 12.0 kcal mol^{-1}. When a sample of the same composition is diluted to 0.5 (w/v) lipid, warmed to 37 °C, and then cooled to 2 °C prior to calorimetric analysis, the major endotherm is strongly diminished and shifted to slightly lower temperatures, and a new, smaller endotherm appears at ~16 °C. The total enthalpy of the endothermic transitions of the sample is now reduced to 8.5 kcal mol^{-1}. Further incubation of this dilute sample at 2 °C for 24 h slightly increases the amplitude of the broad transition at ~22 °C (not shown), and the total enthalpy of transition increases slightly, to 9.1 kcal mol^{-1}. The behavior of 50:50 mixtures of DIPPG and DIPPE therefore resembles that of pure DIPPE in that in both cases, the major endothermic transition of the samples is fully developed only after prolonged low-temperature incubations at high lipid concentrations.

Discussion

The results of previous calorimetric studies of branched-chain phosphatidylcholines (Silvius & McElhaney, 1979; Kannenberg et al., 1983) suggested that these species can exhibit considerable gel-state polymorphism at temperatures near that of the gel to liquid-crystalline phase transition. Recent studies of the properties of straight-chain-saturated phospholipids have demonstrated that many of these species can also form multiple solid phases, some of which may require days or weeks to develop from other solid phases that form more rapidly (Chen et al., 1980; Ruocco & Shipley, 1981a,b; Mantsch et al., 1983; Mulukutla & Shipley, 1984; Serralach et al., 1984). The formation of the subel phase of DPPC, for example, requires incubation near 0 °C for periods of several days (Chen et al., 1980; Füldner, 1981; Ruocco & Shipley, 1982a,b). It is therefore interesting to find that hydrated samples of DIPPC form a gel phase with orthorhombic acyl chain packing after even short periods of incubation at 2 °C. The molar enthalpy of transition of this orthorhombic gel phase to the liquid-crystalline state is comparable to the total molar

enthalpy absorbed by DPPC in its conversion from the subgel phase through the $L_{\beta'}$ and $P_{\beta'}$ phases to the liquid-crystalline state. However, while the orthorhombic phase of DIPPC and the subgel phase of DPPC exhibit some similar properties, the phase diagram for the DIPPC–DPPC system indicates that neither lipid can readily accommodate high proportions of the other species in these phases. The fine details of the structures of the two low-temperature phases are therefore probably significantly different, in spite of the general similarities just noted.

The calorimetric behavior observed with hydrated samples of DIPPE indicates that this lipid can form a number of lamellar "gel" phases, some of which can interconvert only over periods ranging from hours to weeks in the temperature interval 0–36 °C. The most stable phase of DIPPE over the temperature range 0–32 °C, which we will designate as I, forms only slowly on cooling samples from the liquid-crystalline state to 2 °C. Phase I converts at 32.1 °C to an "intermediate" phase, designated as II, which in turn melts to form the liquid-crystalline phase at 35.3 °C. ^{31}P NMR spectra show a greater motional averaging in phase II, compared with phase I, likely due to an increase in the off-axis motion of the phospholipid head group in phase II. The Raman spectroscopic results indicate that phase II contains a high population of gauche conformers, while phase I, as expected for a true "gel-state" phase, does not. In agreement with this observation, the transition from phase I to the intermediate phase II at 32.1 °C is found to be even more endothermic than is the melting of II to the liquid-crystalline phase at 35.3 °C.

As already noted, while solid phase I is apparently the thermodynamically most stable phase of DIPPE below 32 °C, the formation of this phase can be very slow (approximately days to weeks) when samples are incubated at 2 or 25 °C after slow cooling from above 36 °C. The rate of formation of phase I at 2 °C is greatly increased in highly concentrated lipid dispersions, suggesting that extensive bilayer–bilayer interactions facilitate the appearance of this phase. Dilute dispersions of DIPPE, when incubated for periods ranging from a few hours to a few days, appear to form metastable solid phases that convert to the intermediate phase II at 17 °C (for samples incubated for a few hours) or at 23 °C (for samples incubated for ≥12 h). Dilute dispersions of equimolar DIPPG and DIPPE show a similar hindrance to formation of the thermodynamically most stable gel phase when incubated at low temperatures.

The gel phase that forms in bacterial membranes containing branched-chain lipids exhibits a number of unusual properties, including an abnormally high susceptibility to phospholipolytic attack (Bouvier et al., 1981), a wide-angle X-ray diffraction pattern that is less sharp and that indicates a greater average interchain distance than is normally observed for gel-state lipids (Legendre et al., 1980), and a failure of the gel-phase lipid to cause lateral segregation of intramembrane proteins (Haest et al., 1974; Halverson et al., 1978; Legendre et al., 1980; Silvius & McElhaney, 1980b). These anomalous properties are observed even for membranes whose lipids contain essentially a single type of iso- or anteisobranched acyl chain (Silvius & McElhaney, 1980b; Bouvier et al., 1981). This phenomenon is readily understandable in light of our finding that bilayers containing a branched-chain PE, when cooled from the liquid-crystalline state, form the intermediate state much more readily than they form a highly ordered gel phase. Bacterial membranes that are rich in branched-chain PE (or possibly monoglucosyl diglyceride, a lipid with many similar properties) would be expected to form the substantially disordered intermediate phase initially on cooling from the liquid-crystalline state. Additional factors such as lipid compositional heterogeneity, a finite surface charge (which can hinder direct apposition of lipid surfaces), and the presence of membrane protein, which can both hinder direct contact of membrane surfaces and perturb the packing of lipid acyl chains, may effectively preclude the formation of more ordered gel phases in such membranes on any reasonable time scale.

A comparison of the gel to liquid-crystalline phase transition temperatures of several diisopalmitoyl lipids with those of their dielaidoyl counterparts reveals an interesting pattern. The main phase transition temperatures of diisopalmitoyl-PC and -PG (23.1 and 20.7 °C, respectively) lie some 11–12 °C above those of the corresponding dielaidoyl lipids (Silvius, 1982). However, hydrated dispersions of diisopalmitoyl-PE and monoglucosyl diglyceride enter the liquid-crystalline state at 35.3 and 25 °C, respectively, while the corresponding dielaidoyl lipids enter this phase at somewhat higher temperatures [38.1 and 31 °C, respectively (this work: Silvius et al., 1981; Silvius & Gagné, 1984)]. This result demonstrates that to predict how the physical properties of membrane lipids will change in response to a change in fatty acyl composition, one must consider the nature of the lipid polar head groups as well as the structures of the acyl chains.

As a final comparison of the possible functional differences between branched- and straight-chain lipids in bacteria, we consider the relative effects of branched-chain and unsaturated diacyl lipids on the stability of the lamellar liquid-crystalline phase in membranes. It is commonly assumed that the tendency of an amphipathic lipid to form lamellar vs. nonlamellar phases is determined in large part by its "dynamic shape", i.e., by the ratio of the cross-sectional areas occupied by its hydrocarbon chains and its polar head groups (Israelachvili et al., 1977; Cullis & de Kruijff, 1979). It might be expected that isobranched lipids would be more prone than straight-chain lipids to form nonlamellar structures in which the ends of the acyl chains are splayed, such as the hexagonal II or cubic phases. However, DIPPE gives no evidence of a transition to a hexagonal phase up to at least 98 °C, a temperature only 27 °C below the reported value of T_H for DPPE (Seddon et al., 1983). By contrast, the T_H value of dipalmitoleoyl-PE is only 43.5 °C, and that determined for dipalmitelaidoyl-PE is 92.5 °C. By this simple measure, we thus conclude that isobranching of the acyl chains promotes the formation of nonlamellar phases more weakly than does either cis or trans unsaturation. A similar conclusion is reached if we compare the separations between T_H and T_c for for these PE species, which equal 77, 72, 59, and 63 °C, respectively, for dipalmitoleoyl-, dipalmitelaidoyl-, dipalmitoyl-, and diisopalmitoyl-PE (this work; Silvius, 1982; Seddon et al., 1983). By this measure as well, the diisopalmitoyl lipid shows no excpetional tendency to form a nonlamellar phase when compared to straight-chain species of an equal carbon number.

The results of Seddon et al. (1983) have demonstrated that the T_H values measured for saturated di-*n*-acyl and -alkyl PE's rise sharply as the acyl chain length is decreased. A comparison of our measured T_H values for dipalmitoleoyl- and dipalmitelaidoyl-PE with those reported previously for dioleoyl- and dielaidoyl-PE (Cullis & de Kruijff, 1978; Tilcock & Cullis, 1982; Gagné et al., 1985) indicates that this effect of acyl chain length on T_H is similar for other homologous series of PE's as well. The isobranched fatty acyl species found in the membrane lipids of *Bacilli* and various other bacterial genera are predominantly of 16 or fewer carbons (Kaneda, 1977). In light of our results for DIPPE, and considering the effects of

acyl chain length on T_H just described, we predict that the isobranched acyl chains commonly found in the membrane lipids of these bacteria will support the formation of nonlamellar phases less readily than will the 16- and 18-carbon cis-unsaturated species that occur in large amounts in many other bacterial (and eukaryotic) cell membranes.

ACKNOWLEDGMENTS

We thank Drs. Johannes Volwerk and Patricia C. Jost for their suggestion of a useful modification of our phospholipid assay procedure, Dr. Leonard Finegold for providing us with a preprint of his manuscript, and Dr. I. W. Levin for stimulating discussions on Raman spectral assignments of these compounds.

Registry No. DIPPC, 71368-22-4; DIPPE, 97691-67-3; DIPPG, 97691-68-4; DPPC, 2644-64-6; 16c^9-PE, 61599-23-3; 16t^9-PE, 97747-45-0; $(CH_3)_2CH(CH_2)_{12}CO_2H$, 4669-02-7; $Br(CH_2)_{11}OH$, 1611-56-9; $Br(CH_2)_{11}OTHP$, 52056-69-6; $Br(CH_2)_2CH(CH_3)_2$, 107-82-4; $(CH_3)_2CH(CH_2)_{13}OTHP$, 97691-69-5; $(CH_3)_2CH(CH_2)_{13}OH$, 20194-48-3.

REFERENCES

Abidi, T. F., & Yeagle, P. L. (1984) *Biochim. Biophys. Acta 775*, 419.

Akutsu, H., & Kyogoku, Y. (1975) *Chem. Phys. Lipids 14*, 113.

Baer, T. A., & Carney, R. L. (1976) *Tetrahedron Lett.* 4697.

Boerio, P., & Koenig, J. L. (1970) *J. Chem. Phys. 52*, 3425.

Bouvier, P., Op den Kamp, J. A. F., & Van Deenen, L. L. M. (1981) *Arch. Biochem. Biophys. 208*, 242.

Chen, S. C., Sturtevant, J. M., & Gaffney, B. J. (1980) *Proc. Natl. Acad. Sci. U.S.A. 77*, 5060.

Cullis, P. R., & de Kruijff, B. (1978) *Biochim. Biophys. Acta 513*, 31.

Cullis, P. R., & de Kruijff, B. (1979) *Biochim. Biophys. Acta 559*, 399.

Cullis, P. R., de Kruijff, B., & Richards, R. E. (1976) *Biochim. Biophys. Acta 426*, 433.

Dolish, F. R., Fately, W. G., & Bentley, F. F. (1974) *Characteristic Raman Frequencies of Organic Compounds*, Wiley, New York.

Finegold, L., & Singer, A. (1984) *Chem. Phys. Lipids 35*, 291.

Füldner, H. H. (1981) *Biochemistry 20*, 5707.

Gagné, J., Stamatatos, L., Diacovo, T., Hui, S. W., Yeagle, P. L., & Silvius, J. R. (1985) *Biochemistry* (in press).

Gunstone, F. D., & Ismail, I. A. (1967) *Chem. Phys. Lipids 1*, 209.

Haest, C. W. M., Verkleij, A. J., De Gier, J., Scheck, R., Ververgaert, P. H. J. T., & Van Deenen, L. L. M. (1974) *Biochim. Biophys. Acta 356*, 17.

Halverson, C. A., Esser, A. F., & Souza, K. A. (1978) *J. Supramol. Struct. 8*, 129.

Huang, C.-H., Lapides, J., & Levin, I. W. (1982) *J. Am. Chem. Soc. 104*, 5926.

Israelachvili, J. N., Mitchell, D. J., & Ninham, B. W. (1977) *Biochim. Biophys. Acta 470*, 185.

Kaneda, T. (1977) *Microbiol. Rev. 41*, 391.

Kannenberg, E., Blume, A., McElhaney, R. N., & Poralla, K. (1983) *Biochim. Biophys. Acta 733*, 111.

Legendre, S., Letellier, L., & Shechter, E. (1980) *Biochim. Biophys. Acta 602*, 491.

Lowry, R. I., & Tinsley, I. J. (1974) *Lipids 9*, 491.

Mantsch, H. H., Hsi, S. C., Butler, K. W., & Cameron, D. G. (1983) *Biochim. Biophys. Acta 728*, 325.

McElhaney, R. N., & Tourtellotte, M. E. (1969) *Science (Washington, D.C.) 164*, 433.

Miyashita, N., Yoshikoshi, A., & Grieco, P. A. (1977) *J. Org. Chem. 42*, 3772.

Mulukutla, S., & Shipley, G. G. (1984) *Biochemistry 23*, 2514.

O'Leary, T. J., & Levin, I. W. (1984a) *J. Phys. Chem. 88*, 1790.

O'Leary, T. J., & Levin, I. W. (1984b) *J. Phys. Chem. 88*, 4074.

Rodwell, A. W., & Peterson, J. E. (1971) *J. Gen. Microbiol. 68*, 173.

Ruocco, M. J., & Shipley, G. G. (1982a) *Biochim. Biophys. Acta 684*, 59.

Ruocco, M. M., & Shipley, G. G. (1982b) *Biochim. Biophys. Acta 691*, 309.

Saito, Y., & McElhaney, R. N. (1977) *J. Bacteriol. 132*, 485.

Saito, Y., Silvius, J. R., & McElhaney, R. N. (1977) *J. Bacteriol. 132*, 497.

Seddon, J. M., Cevc, G., & Marsh, D. (1983) *Biochemistry 22*, 1280.

Serralach, E. N., de Haas, G. H., & Shipley, G. G. (1984) *Biochemistry 23*, 713.

Silbert, D. F., Ladenson, R. C., & Honegger, J. L. (1973) *Biochim. Biophys. Acta 311*, 349.

Silvius, J. R. (1982) in *Lipid–Protein Interactions* (Jost, P., & Griffith, O. H., Eds.) pp 239–281, Wiley, New York.

Silvius, J. R., & McElhaney, R. N. (1978) *Can. J. Biochem. 56*, 462.

Silvius, J. R., & McElhaney, R. N. (1979) *Chem. Phys. Lipids 24*, 287.

Silvius, J. R., & McElhaney, R. N. (1980a) *Chem. Phys. Lipids 26*, 67.

Silvius, J. R., & McElhaney, R. N. (1980b) *Proc. Natl. Acad. Sci. U.S.A. 77*, 1255.

Silvius, J. R., & Gagné, J. (1984) *Biochemistry 23*, 3232.

Silvius, J. R., Mak, N., & McElhaney, R. N. (1980) *Biochim. Biophys. Acta 597*, 199.

Synder, R. G., Maroncelli, M., Qi, S. P., & Strauss, H. L. (1981) *Science (Washington, D.C.) 214*, 188.

Tilcock, C. P. S., & Cullis, P. (1982) *Biochim. Biophys. Acta 643*, 212.

Van Dijck, P. W. M., de Kruijff, B., van Denen, L. L. M., de Gier, J., & Demel, R. A. (1976) *Biochim. Biophys. Acta 455*, 576.

Verkleij, A. J., & Ververgaert, P. H. J. T. (1975) *Annu. Rev. Phys. Chem. 26*, 101.

Yellin, N., & Levin, I. W. (1977) *Biochim. Biophys. Acta 489*, 177.